REGULAR ARTICLE

blood advances

Landscape of driver mutations and their clinical impacts in pediatric B-cell precursor acute lymphoblastic leukemia

Hiroo Ueno,[1-3,*] Kenichi Yoshida,[1,*] Yusuke Shiozawa,[1,4] Yasuhito Nannya,[1] Yuka Iijima-Yamashita,[2] Nobutaka Kiyokawa,[5] Yuichi Shiraishi,[6] Kenichi Chiba,[6] Hiroko Tanaka,[6] Tomoya Isobe,[4] Masafumi Seki,[4] Shunsuke Kimura,[4,7] Hideki Makishima,[1] Masahiro M. Nakagawa,[1] Nobuyuki Kakiuchi,[1] Keisuke Kataoka,[1,8] Tetsuichi Yoshizato,[1] Dai Nishijima,[2] Takao Deguchi,[9,10] Kentaro Ohki,[5] Atsushi Sato,[11] Hiroyuki Takahashi,[12] Yoshiko Hashii,[13] Sadao Tokimasa,[14] Junichi Hara,[15] Yoshiyuki Kosaka,[16] Koji Kato,[17] Takeshi Inukai,[18] Junko Takita,[3,4] Toshihiko Imamura,[19] Satoru Miyano,[6] Atsushi Manabe,[20] Keizo Horibe,[2] Seishi Ogawa,[1,21,22,†] and Masashi Sanada[2,†]

[1]Department of Pathology and Tumor Biology, Graduate School of Medicine, Kyoto University, Kyoto, Japan; [2]Clinical Research Center, National Hospital Organization Nagoya Medical Center, Nagoya, Japan; [3]Department of Pediatrics, Graduate School of Medicine, Kyoto University, Kyoto, Japan; [4]Department of Pediatrics, Graduate School of Medicine, The University of Tokyo, Tokyo, Japan; [5]Department of Pediatric Hematology and Oncology Research, National Research Institute for Child Health and Development, Tokyo, Japan; [6]Human Genome Center, Institute of Medical Science, University of Tokyo, Tokyo, Japan; [7]Department of Pediatrics, Hiroshima University Graduate School of Biomedical Sciences, Hiroshima, Japan; [8]Division of Molecular Oncology, National Cancer Center Research Institute, Tokyo, Japan; [9]Department of Pediatrics, Mie University Graduate School of Medicine, Tsu, Japan; [10]Children's Cancer Center, National Center for Child Health and Development, Tokyo, Japan; [11]Department of Hematology and Oncology, Miyagi Children's Hospital, Sendai, Japan; [12]Department of Pediatrics, Toho University, Tokyo, Japan; [13]Department of Pediatrics, Osaka University Graduate School of Medicine, Osaka, Japan; [14]Department of Pediatrics, Osaka City University Graduate School of Medicine, Osaka, Japan; [15]Department of Pediatric Hematology/Oncology, Osaka City General Hospital, Osaka, Japan; [16]Department of Hematology/Oncology, Hyogo Prefectural Kobe Children's Hospital, Kobe, Japan; [17]Department of Hematology and Oncology, Children's Medical Center, Japanese Red Cross Nagoya First Hospital, Nagoya, Japan; [18]Department of Pediatrics, University of Yamanashi, Kofu, Japan; [19]Department of Pediatrics, Kyoto Prefectural University of Medicine, Kyoto, Japan; [20]Department of Pediatrics, Hokkaido University Graduate School of Medicine, Sapporo, Japan; [21]Institute for the Advanced Study of Human Biology (WPI-ASHBi), Kyoto University, Kyoto, Japan; and [22]Department of Medicine, Center for Hematology and Regenerative Medicine, Karolinska Institute, Stockholm, Sweden

Key Point

- *TP53* mutations were associated with poor prognosis in NCI high-risk patients but not in SR patients in pediatric B-ALL.

Recent genetic studies using high-throughput sequencing have disclosed genetic alterations in B-cell precursor acute lymphoblastic leukemia (B-ALL). However, their effects on clinical outcomes have not been fully investigated. To address this, we comprehensively examined genetic alterations and their prognostic impact in a large series of pediatric B-ALL cases. We performed targeted capture sequencing in a total of 1003 pediatric patients with B-ALL from 2 Japanese cohorts. Transcriptome sequencing (n = 116) and/or array-based gene expression analysis (n = 120) were also performed in 203 (84%) of 243 patients who were not categorized into any disease subgroup by panel sequencing or routine reverse transcription polymerase chain reaction analysis for major fusions in B-ALL. Our panel sequencing identified novel recurrent mutations in 2 genes (*CCND3* and *CIC*), and both had positive correlations with *ETV6-RUNX1* and hypodiploid ALL, respectively. In addition, positive correlations were also newly reported between *TCF3-PBX1* ALL with *PHF6* mutations. In multivariate Cox proportional hazards regression models for overall survival, *TP53* mutation/deletion, hypodiploid, and *MEF2D* fusions were selected in both cohorts. For *TP53* mutations, the negative effect on overall survival was confirmed in an independent external cohort (n = 466). *TP53* mutation was frequently found in *IGH-DUX4* (5 of 57 [9%]) ALL, with 4 cases having 17p LOH and negatively affecting overall survival therein, whereas *TP53* mutation was not associated with poor outcomes among NCI (National Cancer Institute) standard risk (SR) patients. A conventional treatment approach might be enough, and further treatment intensification might not be necessary, for patients with *TP53* mutations if they are categorized into NCI SR.

Submitted 4 December 2019; accepted 1 September 2020; published online 23 October 2020. DOI 10.1182/bloodadvances.2019001307.

*H.U. and K.Y. contributed equally to this study.

†S.O. and M. Sanada equally led this study.

The data reported in this article have been deposited in the DNA Data Bank of Japan (accession number PRJDB8942).

The full-text version of this article contains a data supplement.

Introduction

B-cell precursor acute lymphoblastic leukemia (B-ALL) accounts for 85% of pediatric ALL and has been categorized into several molecular subgroups according to heterogeneous genomic alterations such as hyperploidy, hypoploidy, *ETV6-RUNX1*, *TCF3-PBX1*, *BCR-ABL1*, *KMT2A*-rearrangements (*KMT2A*r), and Philadelphia (Ph)-like profile.[1,2] Genetic studies using high-throughput sequencing have disclosed landscapes of gene alterations in major subgroups of B-ALL.[3-7] However, the impact of gene mutations and other genetic lesions on clinical outcomes have been investigated in a relatively small number of patients for a limited number of driver mutations and copy number lesions.[8,9] Particularly, genetic profiles and their clinical relevance have been less intensively investigated in rare subtypes of B-ALL, including *TCF3-PBX1*–positive ALL, *ZNF384*, and *MEF2D* fusion-positive ALL, which account for ~7%, 4%, and 2% of pediatric B-ALL, respectively.[10-13] Moreover, different clinical backgrounds of patients frequently complicate the accurate determination of the effects of genetic alterations; for example, generally predicting a poor clinical outcome, *IKZF1* deletions, and Ph-like signatures may not be associated with a shorter overall survival among patients who belong to the National Cancer Institute (NCI) standard risk (SR) category.[9,14] To elucidate precise impacts of genetic alterations, it is instrumental to investigate a large cohort of patients for a comprehensive registry of genetic lesions in B-ALL. In the current study, we elucidated the landscape of driver mutations among 1003 pediatric patients with B-ALL and investigated the significance of driver alterations with regard to the clinical outcomes.

Patients and methods

Patients and risk stratification in treatment protocols

A total of 1003 patients with B-ALL diagnosed between April 2002 and January 2013 were included in this study; 568 and 435 patients were treated according to Japan Association Childhood Leukemia Study Group (JACLS) ALL-02 or Tokyo Children's Cancer Study Group (TCCSG) L04-16 prospective clinical trials, respectively (supplemental Tables 1 and 2; supplemental Figure 1).[15,16] Compared with the clinical background of the entire cohort, sequenced samples, where adequate materials were available for sequencing, had higher white blood cell (WBC) numbers at diagnosis and enriched in the NCI high-risk category. The diagnosis of B-ALL was based on cell morphology and immunophenotype in bone marrow aspirates or peripheral blood at diagnosis. On the basis of conventional karyotyping and reverse transcription polymerase chain reaction assays for known gene fusions routinely performed for all patients at the beginning of enrollment in the therapy protocol, 184 hyperdiploid, 6 hypodiploid, 236 *ETV6-RUNX1*, 95 *TCF3-PBX1*, and 34 *KMT2A*r (17 *KMT2A-AF4*, 10 *KMT2A-ENL*, and 7 *KMT2A-AF9)* cases had been diagnosed. *BCR-ABL1*–positive and infant cases had been excluded from the analysis. Clinical characteristics of the patients are summarized in Table 1. For risk stratification in treatment protocols, patients were provisionally stratified into 3 risk groups based on the patient's age, initial WBC count, and major gene fusions and aneuploidy, including *KMT2A*r, *TCF3-PBX1*, and hypodiploidy. These patients were then reclassified into 4 final risk groups according to the treatment response to initial 7-day prednisolone monotherapy.[16]

Table 1. Characteristics of the patients and univariate associations with overall survival

	n (%)	Hazard ratio for event (95% CI)	*P*
Sample			
Sample size, cases	1003		
Follow up, median (range), y	5.8 (0-18)		
Events			
Induction failure	19 (1.9)		
Relapse	149 (15)		
Death from any cause	95 (9.5)		
Treatment groups*			
SR	303 (30)		
Intermediate risk	451 (45)		
High risk	120 (12)		
Extended high risk	65 (6.5)		
Discontinuation of the protocol treatment	26 (2.6)		
Age, y			<.001
Median (range)	5 (1-18.5)		
1-10	813 (81)	1	
>10	190 (19)	2.6 (1.7-4.0)	
Sex			.3
Female	466 (46)	1	
Male	537 (54)	1.1 (0.8-1.7)	
Leukocyte count in peripheral blood*			<.001
$<50 \times 10^9$/L	819 (82)	1	
$\geq 50 \times 10^9$/L	183 (18)	2.7 (1.8-4.1)	
NCI risk group			<.001
SR	671 (67)	1	
High risk	332 (33)	2.8 (1.9-4.2)	

*Information about final treatment risk and leukocyte count at diagnosis is missing in 38 patients and 1 patient, respectively.

Informed consent was obtained from the patients' guardians according to the Declaration of Helsinki. This study was approved by the institutional review boards at National Hospital Organization Nagoya Medical Center and Kyoto University.

Targeted gene panel sequencing

Genomic DNA was obtained from peripheral blood or bone marrow at diagnosis and subjected to hybridization-based capture by using a SureSelect custom kit (Agilent Technologies), followed by high-throughput sequencing on an Illumina HiSeq 2500 platform. The targeted gene panel included 110 known or putative driver genes in B-ALL and/or target genes of activation-induced cytidine deaminase (supplemental Table 3).[17] In addition, 1484 single-nucleotide polymorphism probes were designed across the entire genome to detect genomic copy numbers, together with an additional 662 probes, which cover the *IGH* enhancer locus to capture *IGH*-involving rearrangements. In sequencing-based copy number analysis, lesions affecting >95% of the entire

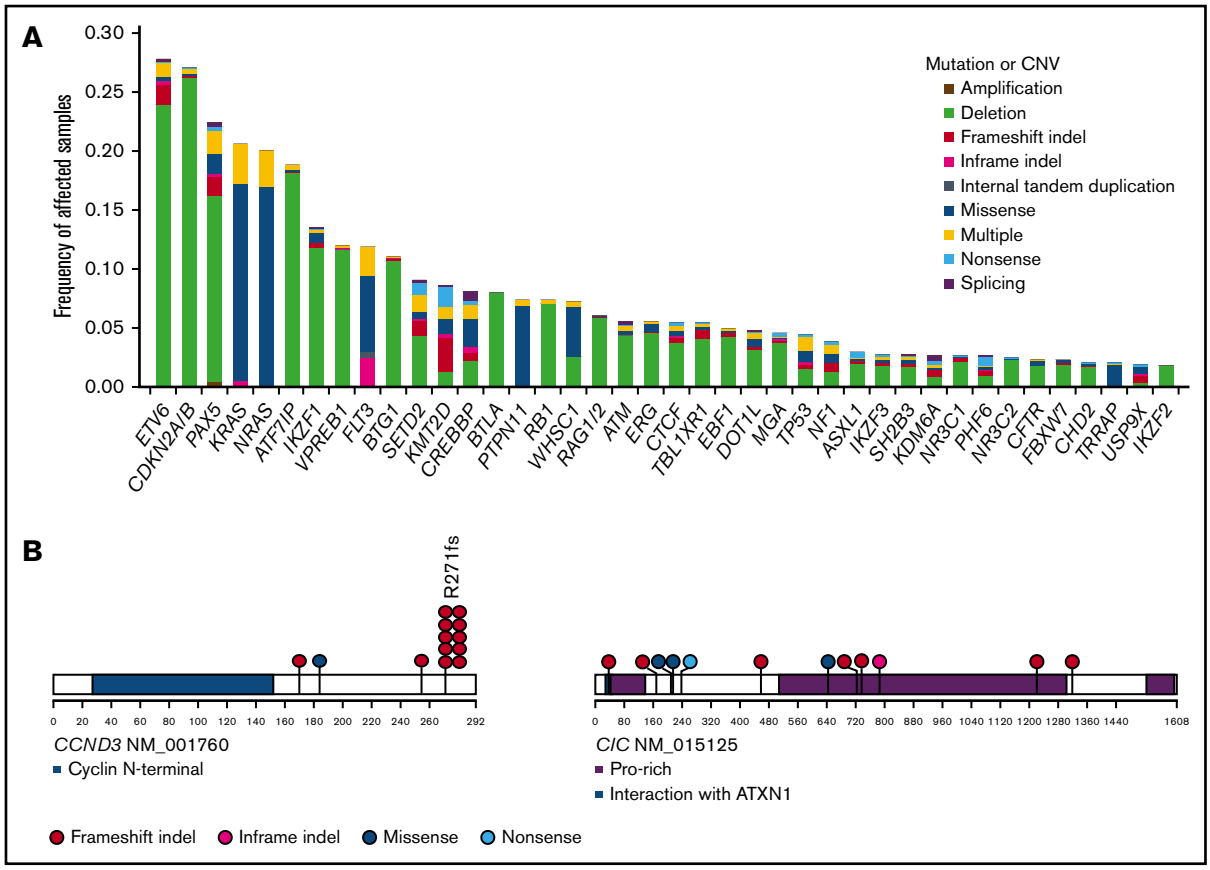

Figure 1. Frequently altered genes and novel driver genes. (A) Frequencies of recurrent mutations and copy number variations (CNVs) identified by targeted capture sequencing. Types of mutations and CNVs are indicated by color. Multiple: more than 1 mutation or mutation accompanied by CNV. (B) Positions and types of somatic mutations in novel driver genes.

chromosome were defined as whole chromosome changes. GenomonPipeline[18] was used for mutation calling with stringent criteria, in which all missense single-nucleotide variants (SNVs) with a variant allele frequency of 0.4 to 0.6 were eliminated as germline variants; the exception was the pathogenic SNVs registered in the Catalogue of Somatic Mutations in Cancer as somatic mutations in hematopoietic and lymphoid neoplasms. Methods of mutation calling, curation of the oncogenic variants, and detection of structural variations are detailed in the supplemental Appendix. Copy number alterations were evaluated by using our in-house pipeline "CNACS."[19] CNACS is a UNIX-based program for sequencing-based copy-number analysis, which is available at (https://github.com/papaemmelab/toil_cnacs).

Transcriptome sequencing and expression array

Gene expression profile was analyzed for 203 patients using Microarray GeneChip Human Genome U133 Plus 2.0 (n = 120) and/or RNA-sequencing (n = 116). RNA samples were extracted from diagnostic specimens using RNeasy Mini Kit. For microarray analysis, GeneChip Operating Software 1.2 (Affymetrix) and GeneSpring GX 13.1 software (Agilent Technologies) were used. Construction of an RNA-sequencing library was performed by using an NEBNext Ultra RNA Library Prep Kit for Illumina according to the manufacturer's instructions. Mapped reads were counted for each gene using our in-house GenomonExpression pipeline. Gene expression levels were normalized by using the R package "DESeq2" and were subjected to clustering analysis to detect Ph-like and *ETV6-RUNX1*–like ALL. Fusion transcripts were detected by Genomon version 2.3.4. Methods of detection of Ph-like and *ETV6-RUNX1*–like ALL and identification of fusion transcripts are detailed in the supplemental Appendix.

Statistical analysis

Associations of genetic alterations with B-ALL subgroups and clinical factors were analyzed by using the Fisher's exact test or the Wilcoxon rank sum test. Multiple testing was adjusted by calculating q values using Benjamini-Hochberg's method, in which $q < 0.1$ was considered statistically significant. Event-free and overall survivals were estimated by using the Kaplan-Meier method. An event was defined as either a failure to achieve remission, a relapse after remission, or any cause of death. Univariate analyses were performed by using the Cox proportional hazards regression model, in which $P < .05$ was considered statistically significant. Using these variables with NCI risk criteria and adjustment to treatment intensity, multivariate analyses were conducted based on the Cox proportional hazards model, and optimal combination of covariates was selected with the least absolute shrinkage and selection operator using R package

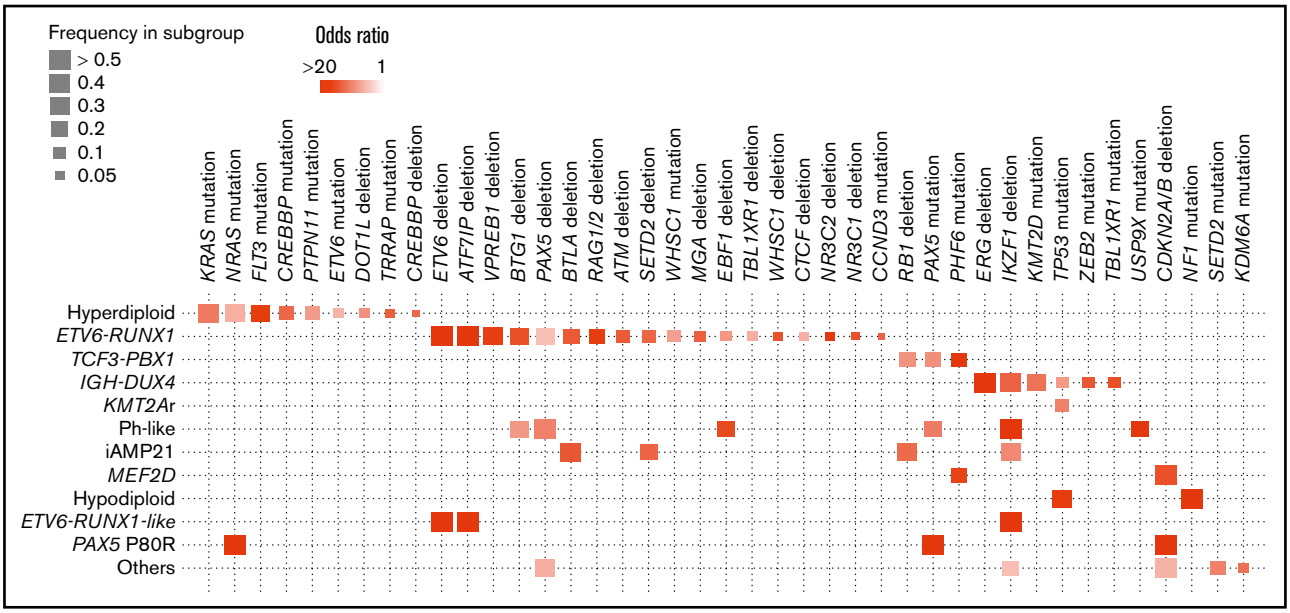

Figure 2. Positive correlations between genetic alterations with disease subgroups. Statistically significant pairwise relationships ($q < 0.1$) for cooccurrence between a genetic alteration and a disease subgroup. Color gradient indicates odds ratio, and size of boxes show frequency of affected samples in each subgroup.

"glmnet" for overall survival. All analyses were performed by using R software (www.r-project.org).

Results

Panel sequencing of 1003 B-ALL SNVs

In total, we detected 1300 SNVs (median, 1 per patient; range, 0-8) and 398 indels (median, 0 per patient; range, 0-5), which frequently affected transcription factors (*ETV6*, *PAX5*, and *IKZF1*), epigenetic regulators (*ATF7IP*, *SETD2*, *KMT2D*, and *CREBBP*), cell cycle regulators (*CDKN2A/B*, *BTG1,* and *RB1*), RAS pathway genes (*KRAS, NRAS,* and *PTPN11*), and *FLT3* (Figure 1A; supplemental Figure 2; supplemental Tables 4 and 5). Novel recurrent mutations were identified in 2 genes, *CCND3* (n = 13) and *CIC* (n = 5) (Figure 1B). *CCND3* were mutated in 13 cases, 8 of which were positive for *ETV6-RUNX1*. Although recurrent *CCND3* mutations have recently been reported in *KMT2A*r AML as well as non-Hodgkin lymphomas, none of the cases with *KMT2A*r ALL carried these mutations.[20,21] As is the case with mutations in lymphomas and *KMT2A*r AML, *CCND3* mutations exhibited a prominent mutational hotspot at R271. Except for 1 missense mutation, all *CCND3* mutations caused a truncating protein lacking the PEST domain, which is known to be involved in casein-mediated degradation of this cyclin.[22] Thus, the consequence of these mutations would be an elevated expression of this cyclin. *CIC* encodes a transcriptional repressor containing a Sox-like high-mobility group box, which was mutated in 4 of 9 patients with hypodiploid ALL (Fisher's exact test, $P = 1.5 \times 10^{-8}$), showing multiple discrete mutations in 3 cases (converging mutations); this finding suggests strong positive selection of *CIC*-mutated cells, as seen in lower grade gliomas.[23]

Some of mutational targets, including *ETV6, CDKN2A/B*, *PAX5*, *IKZF1*, and *ERG*, were more commonly affected by focal deletions, which were sensitively detected by sequencing-based copy number analysis (Figure 1A; supplemental Figure 3). In addition to these focal events, whole chromosomal events were frequently observed; according to sequencing-based analysis, we found 307 hyperdiploid and 9 hypodiploid (7 were near-haploid and 2 were low-hypodiploid) cases, as well as 13 iAMP21-positive cases (supplemental Appendix). In accordance with a previous report,[24] a substantial number of cases with hyperdiploid ALL were overlooked in conventional metaphase karyotyping; in the latter analysis, only 57% (n = 174 of 307) of all hyperdiploid cases were detected (supplemental Figure 4A). In particular, hyperdiploid cases with lower peripheral WBC counts at diagnosis tended to escape more from metaphase karyotyping (supplemental Figure 4B). Notably, patients with hyperdiploid ALL detected by sequencing-based analysis alone exhibited an overall survival almost identical to that of other hyperdiploid cases detected by metaphase karyotyping (supplemental Figure 4C). We found 9 cases apparently showing hypodiploid on the basis of extensive LOH in the majority of chromosome; 2 of these cases exhibited a hyperdiploid karyotype, and 2 other cases had a normal karyotype (supplemental Figure 5). Breakpoints of *IGH*-involving translocations were successfully captured in 71 patients, which most frequently affected *DUX4* (n = 57 [5.7%]), followed by *EPOR* (n = 7 [0.6%]), *CRLF2* (n = 4 [0.4%]), *BCL2* (n = 2 [0.2%]), and *MYC* (n = 1 [0.1%]) (supplemental Table 4).

Correlation between genetic alteration and disease subgroup

On the basis of panel sequencing, 760 of 1003 B-ALL cases were classified into 10 nonoverlapping subgroups, either of hyperdiploid (n = 307 [31%]) or hypodiploid (n = 9 [1%]) karyotypes; *ETV6-RUNX1* (n = 236 [23%]), *TCF3-PBX1* (n = 95 [10%]), and *IGH-DUX4* (n = 57 [6%]) fusions; *PAX5* p.Pro80Arg (n = 4 [0.4%]) and *IKZF1* p.Asn159Tyr (n = 3 [0.3%]) mutations; or *KMT2A*r (n = 34 [3%]), iAMP21 (n = 13 [1%]), and *BCL2/MYC* (n = 2 [0.2%]) (supplemental Figure 6). In accordance with a previous report,[1]

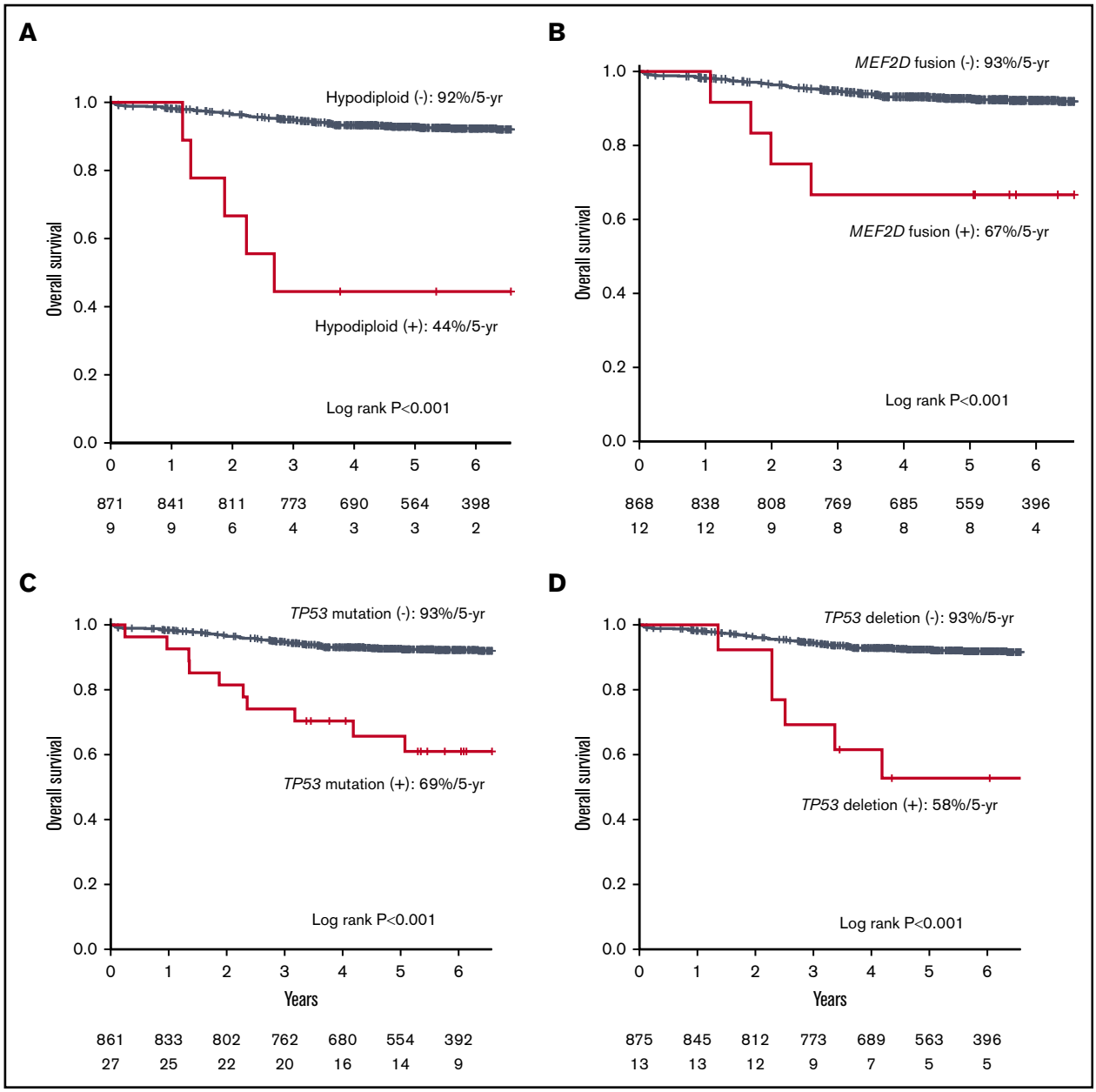

Figure 3. Kaplan-Meier curves for hypodiploid, *MEF2D* fusion, *TP53* mutation, and *TP53* deletion in the Japanese cohort. Kaplan-Meier curves of overall survival for individuals in the Japanese cohort with or without hypodiploid (A), *MEF2D* fusion (B), *TP53* mutation (C), and *TP53* deletion (D).

PAX5 p.P80R and *IKZF1* N159Y (novel subgroup-defining SNVs) were rare in our pediatric cohort. Of the remaining 243 cases, high-quality RNA was available in 203 (84%) for gene expression analysis to identify cases with Ph-like or *ETV6-RUNX1*–like phenotype and other fusions, using transcriptome sequencing (n = 116) and/or array-based gene expression analysis (n = 120) (supplemental Figure 7). Twenty-one patients were classified as Ph-like ALL. Transcriptome sequencing also revealed *ETV6-RUNX1*–like profile (n = 6) and *ZNF384* (n = 15), *MEF2D* (n = 12), and *NUTM1* (n = 4) fusions, including novel fusion partners (*MEF2D-PYGO2* and *NUTM1-ATAD5*) (supplemental Table 6).

Altogether, we classified 880 B-ALL cases into 15 discrete subtypes; genetic features of these subtypes were further investigated, focusing on 50 recurrent alterations that were detected in at least 10 patients (supplemental Table 7). We first investigated a significant enrichment of these genetic lesions within each B-ALL subtype. Deletions in hypodiploid ALL were excluded from the analysis, because almost all driver genes were deleted in this subtype. In total, we found 62 significant enrichment events, $q < 0.1$ (Figure 2). Most common driver changes were significantly enriched in one or more disease subgroups. Although most of these correlations had previously been reported, we newly identified a significant enrichment of *PHF6* and *PAX5* mutations in *TCF3-PBX1* ALL and an *SETD2* deletion in iAMP21 ALL. In addition, *IKZF1* deletions were significantly enriched in the *IGH-DUX4*, Ph-like, iAMP21, and *ETV6-RUNX1*–like subgroups. Recently,

Table 2. Selected variables by using the least absolute shrinkage and selection operator in a Cox proportional hazards multiple regression model

JACLS		TCCSG	
Selected variables	**Hazard ratio**	**Selected variables**	**Hazard ratio**
TP53 deletion	14	*TP53* deletion	3.8
Hypodiploid	8.4	Hypodiploid	14
MEF2D	4.4	*MEF2D*	5.3
TP53 mutation	1.3	*TP53* mutation	2.6
IKZF1 deletion	1.1	Prednisone poor response	1.5
IGH-DUX4	1.7	*JAK2* mutation	2.4
NCI HR	1.7	Ph-like	2.7
TCF3-PBX1	2.2	*KMT2A*r	3.0
PAX5 mutation	2.5		
iAMP21	2.7		

IKZF1^{plus} has been reported to be a very poor prognostic factor.[25] We therefore further analyzed the corelationship of the *IKZF1*^{plus} pattern with genetic subgroups. Among 81 cases with *IKZF1* deletion, 31 cases fulfilled the *IKZF1*^{plus} definition, and Ph-like ALL was enriched in *IKZF1*^{plus} (Fisher's exact test, $P = .002$) (supplemental Appendix; supplemental Table 8).

Clinical effects of genetic alterations

We examined the effects of 50 genetic lesions and 8 subtypes detected in at least 10 cases on survival in the JACLS and TCCSG cohorts. As in the correlation analysis, all deletions in hypodiploid ALL were also excluded in the survival analysis. In univariate analyses, 10 variables were significantly associated with shorter overall survival in each cohort (supplemental Table 9). We next performed multivariate Cox proportional hazard models in each cohort using these 10 variables and factors relevant to treatment stratification: NCI category, prednisone poor response, hypodiploidy, *TCF3-PBX1*, and *KMT2A*r. After adjustment to treatment intensity, *TP53* mutation, *TP53* deletion, hypodiploidy, and *MEF2D* fusions were selected in the model in both the JACLS and the TCCSG cohort (Figure 3; Table 2; supplemental Table 10). To confirm the finding, we analyzed whole-exome sequencing data of 466 patients with B-ALL publicly available from the TARGET (Therapeutically Applicable Research to Generate Effective Treatments) project (AALL0331 and AALL0232), in which paired germline control samples were sequenced in all cases. Clinical backgrounds were almost the same as those in the Japanese cohorts, suggesting that the TARGET cohort was suitable for verification (supplemental Table 11). In this external data set, *TP53* mutation was associated with shorter overall survival (log-rank test, $P < .001$); however, *TP53* deletion was not associated with shorter event-free or overall survival in the TARGET cohort (supplemental Figure 8; supplemental Table 12).

In the total 1003 cases, 36 *TP53* mutations were identified in 30 patients: 22 missense and 2 nonsense mutations, as well as 7 frameshift and 5 in-frame indels (supplemental Tables 13-15). Among them, 11 cases (37%) were accompanied by 17p LOH. As for pathogenicity, 21 of 22 missense mutations are believed to result in complete (n = 19) or partial (n = 2) loss of transcriptional activity in the International Agency for Research on Cancer TP53 database[26]; the remaining mutation (p.Y236N) was predicted to be damaging by PolyPhen2, SIFT,[27] and M-CAP.[28] The size of the *TP53*-mutated clones exhibited a substantial difference among patients (0.03-1, with a median of 0.3), and from the view of this distribution, most of the *TP53* mutations were considered to be somatic (supplemental Figure 9). The clone size of *TP53* mutations did not significantly correlate with poor prognosis or high NCI risk (supplemental Figure 10).

In terms of disease subtype, *TP53* mutations were enriched in hypodiploid (3 of 9 [33%]), *KMT2A*r (4 of 34 [12%]), and *IGH-DUX4* (5 of 57 [9%]) (Figures 2 and 4A). Of note, *TP53* mutations predicted a dismal prognosis even in *IGH-DUX4* fusion-positive ALL, which has otherwise been associated with favorable clinical outcomes (Figure 4B). In *IGH-DUX4* fusion-positive ALL, *TP53* mutations were frequently accompanied by 17p LOH (n = 4 of 5); only 7 of the other 25 *TP53* mutated cases harbored 17p LOH (Fisher's exact test, $P = .047$). In NCI-SR patients, the presence of a *TP53* mutation did not predict poor prognosis (log-rank test, $P = .9$) (Figure 4C), and the same was true in the TARGET cohort (log-rank test, $P = .6$).

Discussion

During the past decade, a complete registry of driver alterations in pediatric B-ALL have been clarified by using advanced sequencing technologies. However, exact frequencies and combinations of these mutations, as well as their effects on clinical outcomes, have not been fully elucidated in a larger cohort of patients, including rare subtypes of B-ALL. Enrolling >1000 cases, our study represents one of the largest genetic analyses on pediatric B-ALL, through which we have revealed a complete landscape of major genetic alterations in this common pediatric malignancy and their clinical effects.

Through the analysis, different subtypes of B-ALL were shown to be characterized by a unique pattern of driver alterations, including previously unknown correlations between *ETV6-RUNX1* ALL with *CCND3* mutations, hypodiploid ALL with *CIC* mutations, and *TCF3-PBX1* ALL with *PHF6* and *PAX5* mutations. The unique enrichment of mutations suggests a discrete pathophysiology of different B-ALL subtypes, which might promote our understanding of the molecular pathogenesis of B-ALL. Our results also support the usefulness of clinical application of next-generation sequencing for accurate diagnosis in pediatric B-ALL; it allows for detection of copy number change, focal deletion, and SNVs in the single platform.

Except for the germline *TP53* mutations and somatic *TP53* mutations at relapse,[29,30] the clinical significance of *TP53* mutations at diagnosis has not fully been investigated in pediatric ALL. In our cohort, *TP53* mutations were more commonly found in hypodiploid, *KMT2A*r, and *IGH-DUX4* ALL. Particularly, even in *IGH-DUX4* ALL, which generally predicts a favorable prognosis, most cases with *TP53* mutations exhibited a dismal outcome in this cohort. This finding needs to be validated in an external cohort, but these results may suggest the need for novel therapeutic approaches in these patients. Of particular note, however, is that the negative effects of *TP53* mutations were not observed in NCI-SR patients, suggesting that for these individuals, the presence of *TP53* mutations may not necessarily predict a poor prognosis, and they therefore could be successfully treated with conventional protocols with no further intensification.

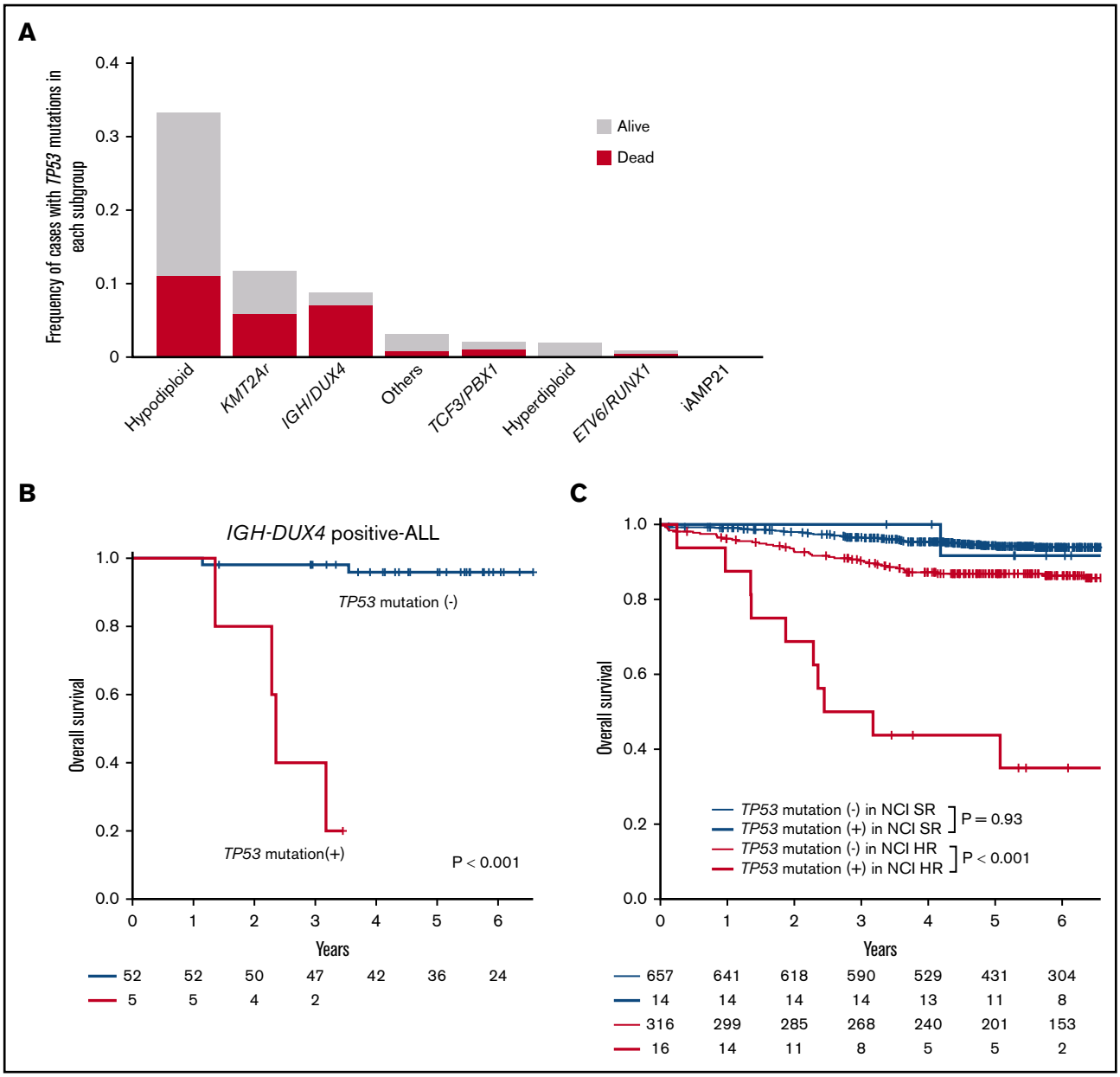

Figure 4. Prevalence and prognostic impact of *TP53* mutations. (A) Frequencies of *TP53* mutations in each subgroup. Outcomes are indicated by colors. (B) Kaplan-Meier curves of overall survival for individuals with and without *TP53* mutations in *IGH-DUX4* positive-ALL. (C) Kaplan-Meier curves of overall survival among patients with or without *TP53* mutations stratified with NCI criteria.

In addition, the negative prognostic impact of *TP53* deletion was not validated in the TARGET cohort. Most of the *TP53* deletions (n = 23 of 26) were consequences of deletion involving >50% of chromosome 17p. In the United Kingdom cohort, 17p abnormality was associated with poor outcome, but only for patients without one of the good-risk abnormalities of *ETV6-RUNX1* and high hyperdiploidy.[31] In the TARGET cohort, *TP53* deletion was not associated with poor outcome even after excluding these good-risk subgroups (data not shown). Although *TP53* mutations were frequently (37%) accompanied by 17pLOH, the functional relevance of exclusive *TP53* deletions remains unclear.

In conclusion, we comprehensively elucidated genetic alterations and their clinical significance in pediatric B-ALL. Our study should provide an essential guide for diagnosis, prediction of prognosis, and optimal therapy using a genomics-based approach in pediatric patients with B-ALL.

Acknowledgments

The authors thank Tomomi Ishida, Mayumi Kibe, Miho Yamada, Mika Fuyama, and Kanako Okada for excellent technical assistance. They also thank all the staffs in the Organization for Supporting Clinical Research data center for data management and the physicians who registered patients in the JACLS ALL-02 or TCCSG L04-16 clinical trials. The authors also express their deep gratitude to those patients who have provided consent to use their biological materials and clinical data.

This work was supported by Grant-in-Aid for Practical Research for Innovative Cancer Control (16ck0106066h0003, 17ck0106253h0001, and 18ck0106253h0002) (M. Sanada), the Program for an Integrated Database of Clinical and Genomic Information (17kk0205005h0002 [K.H.] and 18kk0205005s0203 [S.O.]), and the Program for a Cancer Research and Therapeutic Evolution (18cm0106501h0003JP) (S.O.) from the Japan Agency for Medical Research and Development, Scientific Research from the Japan Society for the Promotion of Science (17K10136) (M. Sanada), and the Takeda Science Foundation (M. Sanada). It was also supported by Grants for Clinical Cancer Research from the Ministry of Health, Labour and Welfare of Japan: H14-Koka(Gan)-031, H15-Koka(Gan)-024, H16-GanRinsho-004, H17-GanRinsho-004, H20-GanRinsho-Ippan-017, and H23-GanRinsho-Ippan-014 (K.H.). This research used computational resources of the K computer provided by the RIKEN Advanced Institute for Computational Science through the HPCI System Research project (hp150232) (S.O.).

Authorship

Contribution: K.H., S.O., and M. Sanada designed the study; Y.I.-Y., T.D., N. Kiyokawa, K.O., A.S., H. Takahashi, Y.H., S.T., J.H., Y.K., K. Kato, T. Inukai, J.T., T. Imamura, A.M., K.H., and M. Sanada collected clinical data and DNA specimens; H.U. and Y.I.-Y. performed sample preparation and sequencing; H.U., K.Y., Y. Shiozawa, Y.N., Y.I.-Y., Y. Shiraishi, K.C., H. Tanaka, N. Kiyokawa, T. Isobe, M. Seki, S.K., H.M., M.M.N., N. Kakiuchi, K. Kataoka, T.Y., D.N., and S.M. analyzed data; H.U., S.O., and M. Sanada wrote the manuscript; and all the authors reviewed and approved the final manuscript.

Conflict-of-interest disclosure: The authors declare no competing financial interests.

ORCID profiles: H.U., 0000-0001-7617-1672; H. Tanaka, 0000-0001-9634-8922; T. Isobe, 0000-0002-3487-3307; M. Seki, 0000-0003-4671-7026; S.K., 0000-0002-2158-467X; M.M.N., 0000-0002-6420-2555; N. Kakiuchi, 0000-0003-4893-5414; K. Kataoka, 0000-0002-8263-9902; T.Y., 0000-0003-4283-2983; T.D., 0000-0001-9932-4299; H. Takahashi, 0000-0001-8763-0280; J.T., 0000-0002-2452-6520; T. Imamura, 0000-0002-5727-4470; K.H., 0000-0002-6251-6059; S.O., 0000-0002-7778-5374; M. Sanada, 0000-0003-0666-1996.

Correspondence: Seishi Ogawa, Department of Pathology and Tumor Biology, Graduate School of Medicine, Kyoto University, Yoshida-Konoe-cho, Sakyo-ku, Kyoto 606-8501, Japan; e-mail: sogawa-tky@umin.ac.jp; or Masashi Sanada, Clinical Research Center, National Hospital Organization Nagoya Medical Center, 4-1-1, Sannomaru, Naka-ku Nagoya-shi, Aichi, 460-0001, Japan; e-mail: masashi.sanada@nnh.go.jp.

References

1. Gu Z, Churchman ML, Roberts KG, et al. PAX5-driven subtypes of B-progenitor acute lymphoblastic leukemia. *Nat Genet*. 2019;51(2):296-307.
2. Pui CH, Relling MV, Downing JR. Acute lymphoblastic leukemia. *N Engl J Med*. 2004;350(15):1535-1548.
3. Holmfeldt L, Wei L, Diaz-Flores E, et al. The genomic landscape of hypodiploid acute lymphoblastic leukemia. *Nat Genet*. 2013;45(3):242-252.
4. Papaemmanuil E, Rapado I, Li Y, et al. RAG-mediated recombination is the predominant driver of oncogenic rearrangement in ETV6-RUNX1 acute lymphoblastic leukemia. *Nat Genet*. 2014;46(2):116-125.
5. Paulsson K, Lilljebjörn H, Biloglav A, et al. The genomic landscape of high hyperdiploid childhood acute lymphoblastic leukemia. *Nat Genet*. 2015;47(6):672-676.
6. Yasuda T, Tsuzuki S, Kawazu M, et al. Recurrent DUX4 fusions in B cell acute lymphoblastic leukemia of adolescents and young adults [published correction appears in *Nat Genet*. 2016;48(12):1591]. *Nat Genet*. 2016;48(5):569-574.
7. Zhang J, McCastlain K, Yoshihara H, et al; St. Jude Children's Research Hospital–Washington University Pediatric Cancer Genome Project. Deregulation of DUX4 and ERG in acute lymphoblastic leukemia. *Nat Genet*. 2016;48(12):1481-1489.
8. Malinowska-Ozdowy K, Frech C, Schönegger A, et al. KRAS and CREBBP mutations: a relapse-linked malicious liaison in childhood high hyperdiploid acute lymphoblastic leukemia. *Leukemia*. 2015;29(8):1656-1667.
9. Chen IM, Harvey RC, Mullighan CG, et al. Outcome modeling with CRLF2, IKZF1, JAK, and minimal residual disease in pediatric acute lymphoblastic leukemia: a Children's Oncology Group study. *Blood*. 2012;119(15):3512-3522.
10. Asai D, Imamura T, Yamashita Y, et al; Japan Association of Childhood Leukemia Study (JACLS) & Children's Cancer and Leukemia Study Group (CCLSG). Outcome of TCF3-PBX1 positive pediatric acute lymphoblastic leukemia patients in Japan: a collaborative study of Japan Association of Childhood Leukemia Study (JACLS) and Children's Cancer and Leukemia Study Group (CCLSG). *Cancer Med*. 2014;3(3):623-631.
11. Hirabayashi S, Ohki K, Nakabayashi K, et al; Tokyo Children's Cancer Study Group (TCCSG). ZNF384-related fusion genes define a subgroup of childhood B-cell precursor acute lymphoblastic leukemia with a characteristic immunotype. *Haematologica*. 2017;102(1):118-129.
12. Ohki K, Kiyokawa N, Saito Y, et al; Tokyo Children's Cancer Study Group (TCCSG). Clinical and molecular characteristics of *MEF2D* fusion-positive B-cell precursor acute lymphoblastic leukemia in childhood, including a novel translocation resulting in *MEF2D-HNRNPH1* gene fusion. *Haematologica*. 2019;104(1):128-137.
13. Gu Z, Churchman M, Roberts K, et al. Genomic analyses identify recurrent MEF2D fusions in acute lymphoblastic leukaemia. *Nat Commun*. 2016;7:13331.
14. Roberts KG, Reshmi SC, Harvey RC, et al. Genomic and outcome analyses of Ph-like ALL in NCI standard-risk patients: a report from the Children's Oncology Group. *Blood*. 2018;132(8):815-824.
15. Hasegawa D, Imamura T, Yagi K, et al. Risk-adjusted therapy of acute lymphoblastic leukemia can optimize the indication of stem cell transplantation and cranial irradiation: results of Japan Association Childhood Leukemia Study Group (JACLS) Protocol ALL-02. *Blood*. 2016;128:3973.

16. Takahashi H, Kajiwara R, Kato M, et al. Treatment outcome of children with acute lymphoblastic leukemia: the Tokyo Children's Cancer Study Group (TCCSG) Study L04-16. *Int J Hematol*. 2018;108(1):98-108.

17. Swaminathan S, Klemm L, Park E, et al. Mechanisms of clonal evolution in childhood acute lymphoblastic leukemia. *Nat Immunol*. 2015;16(7):766-774.

18. Shiraishi Y, Sato Y, Chiba K, et al. An empirical Bayesian framework for somatic mutation detection from cancer genome sequencing data. *Nucleic Acids Res*. 2013;41(7):e89.

19. Yoshizato T, Nannya Y, Atsuta Y, et al. Genetic abnormalities in myelodysplasia and secondary acute myeloid leukemia: impact on outcome of stem cell transplantation. *Blood*. 2017;129(17):2347-2358.

20. Schmitz R, Young RM, Ceribelli M, et al. Burkitt lymphoma pathogenesis and therapeutic targets from structural and functional genomics. *Nature*. 2012; 490(7418):116-120.

21. Matsuo H, Yoshida K, Fukumura K, et al. Recurrent *CCND3* mutations in *MLL*-rearranged acute myeloid leukemia. *Blood Adv*. 2018;2(21):2879-2889.

22. Rogers S, Wells R, Rechsteiner M. Amino acid sequences common to rapidly degraded proteins: the PEST hypothesis. *Science*. 1986;234(4774): 364-368.

23. Suzuki H, Aoki K, Chiba K, et al. Mutational landscape and clonal architecture in grade II and III gliomas. *Nat Genet*. 2015;47(5):458-468.

24. Nygaard U, Larsen J, Kristensen TD, et al. Flow cytometric DNA index, G-band karyotyping, and comparative genomic hybridization in detection of high hyperdiploidy in childhood acute lymphoblastic leukemia. *J Pediatr Hematol Oncol*. 2006;28(3):134-140.

25. Stanulla M, Dagdan E, Zaliova M, et al; International BFM Study Group. IKZF1^{plus} defines a new minimal residual disease-dependent very-poor prognostic profile in pediatric B-cell precursor acute lymphoblastic leukemia. *J Clin Oncol*. 2018;36(12):1240-1249.

26. Kato S, Han SY, Liu W, et al. Understanding the function-structure and function-mutation relationships of p53 tumor suppressor protein by high-resolution missense mutation analysis. *Proc Natl Acad Sci U S A*. 2003;100(14):8424-8429.

27. Kumar P, Henikoff S, Ng PC. Predicting the effects of coding non-synonymous variants on protein function using the SIFT algorithm. *Nat Protoc*. 2009; 4(7):1073-1081.

28. Jagadeesh KA, Wenger AM, Berger MJ, et al. M-CAP eliminates a majority of variants of uncertain significance in clinical exomes at high sensitivity. *Nat Genet*. 2016;48(12):1581-1586.

29. Qian M, Cao X, Devidas M, et al. TP53 germline variations influence the predisposition and prognosis of B-cell acute lymphoblastic leukemia in children. *J Clin Oncol*. 2018;36(6):591-599.

30. Hof J, Krentz S, van Schewick C, et al. Mutations and deletions of the TP53 gene predict nonresponse to treatment and poor outcome in first relapse of childhood acute lymphoblastic leukemia. *J Clin Oncol*. 2011;29(23):3185-3193.

31. Moorman AV, Ensor HM, Richards SM, et al. Prognostic effect of chromosomal abnormalities in childhood B-cell precursor acute lymphoblastic leukaemia: results from the UK Medical Research Council ALL97/99 randomised trial. *Lancet Oncol*. 2010;11(5):429-438.